Agricultural Water Management 306 (2024) 109175

Contents lists available at ScienceDirect

Agricultural Water Management

journal homepage: www.elsevier.com/locate/agwat

Regional-scale evaluation of tertiary irrigation system in Muda Irrigation Scheme from space

Aliya Mhd Zahir [a,b], Hiroaki Somura [a,*], Toshitsugu Moroizumi [a]

[a] Graduate School of Environmental and Life Science, Okayama University, 3-1-1 Tsushima-naka, Kita-ku, Okayama 700-8530, Japan

[b] Department of Irrigation and Drainage, Ministry of Energy Transition and Water Transformation Malaysia, Persiaran Rimba Permai, Cyber 8, Cyberjaya, Selangor 63000, Malaysia

ARTICLE INFO

Handling Editor: J.E. Fernández

Keywords:
Water management
Remote sensing
Irrigation performance
Irrigation system
Earth observation data
Muda Irrigation Scheme

ABSTRACT

A tertiary irrigation system is essential for efficient water management in large-scale irrigation scheme and requires regular evaluation to understand their effectiveness. The current water balance method for tertiary irrigation system evaluation requires extensive data, making continuous monitoring over vast areas unfeasible. A better approach using geospatial data from the Google Earth Engine (GEE) is introduces to evaluate the efficiency of tertiary irrigation systems on a regional scale, aiding water management strategies. This study aims to (1) define the rice cultivation boundary for accurate data collection and (2) quantitatively evaluate irrigation system performance using specific indicators. Remote sensing evapotranspiration (RS-ET) and yield derived from Normalized Difference Vegetation Index (NDVI) were collected within rice cultivation boundary across 60 irrigation blocks, including 14 blocks equipped with tertiary irrigation system in Region II of the Muda Irrigation Scheme. Three irrigation system performance indicators (equity, adequacy, and water productivity) were used as a key metric in over four rice-growing seasons to evaluate tertiary irrigation system. Results reveal that tertiary irrigation system performance varies with the current three-phase water management strategy. Equity performance was highest during the off-season, particularly in phase 1 (2–8 %). Adequacy was moderate across all phases and seasons (median: 0.6–0.67), while water productivity showed consistent strength in phases 1 and 3, with fluctuations in phase 2, across seasons. This study underscores the cost-effectiveness and efficiency of using geospatial data from space for continuous regional-scale monitoring, highlighting areas for improvement in the current water management strategy.

1. Introduction

A tertiary irrigation system is the most localized level of an irrigation network, responsible for delivering water directly from the secondary system to agricultural plots within an irrigation block. This system is crucial for efficient water distribution from available resources to individual farmers and their fields. Timely and sufficient water from tertiary irrigation system increases crop productivity through the likelihood of agricultural practices, thus contributes to high yields (Mohsen Aly et al., 2013; Ragab et al., 2019; Seiro et al., 2016; Vandersypen et al., 2006). The significance of monitoring tertiary irrigation system for rice paddy is increasing, where sufficient water stands out as the primary factor influencing yield (Cai and Sharma, 2010), especially when governing bodies delegate field operations and management of tertiary canal to farmers (Mohsen Aly et al., 2013; Ragab et al., 2019). To fully understand the effectiveness of the tertiary irrigation system, continuous monitoring of its operation and regular evaluation of its performance are required. While past evaluations have focused on water delivery performance through discharge and water withdrawal from irrigation practices (Mohammadi et al., 2019; Mohsen Aly et al., 2013; Syed et al., 2021), they primarily addressed the water supply aspect, overlooking field-level water requirements. This information gap can lead to water shortages and ineffective use of tertiary irrigation system (Mohsen Aly et al., 2013; Ragab et al., 2019; Vandersypen et al., 2006).

Although information on water supply and demand is necessary for a comprehensive evaluation of tertiary irrigation system, obtaining this information for continuous monitoring of a large-scale irrigation scheme is a challenge and requires alternatives approach. Large-scale irrigation

* Corresponding author.
E-mail addresses: aliyazahir@s.okayama-u.ac.jp, aliya@water.gov.my (A.M. Zahir), somura@okayama-u.ac.jp (H. Somura), morot@okayama-u.ac.jp (T. Moroizumi).

https://doi.org/10.1016/j.agwat.2024.109175
Received 20 February 2024; Received in revised form 6 November 2024; Accepted 12 November 2024
Available online 22 November 2024

scheme covers extensive areas and involve significant uses of water resources. Assessing tertiary irrigation system within this context helps ensure identifying nonperforming water management strategy across the entire scheme based on efficient water distribution, and utilization. By evaluating the performance of tertiary irrigation system at this scale, it becomes possible to identify areas of inefficiency or wastage, leading to more effective water management strategies. To evaluate the performance of the tertiary irrigation system, a water balance method had been used by previous researchers (Kitamura, 1990; Ragab et al., 2019; Vandersypen et al., 2006; Yashima, 1987, 1982). Water balance study relies on various factors related to water supply and demand within irrigation blocks such as details of inflows and outflows, including changes in the soil content at the point where the information is measured, makes it representative only for the targeted irrigation blocks and temporarily during the evaluation period (Kitamura, 1990; Ragab et al., 2019; Vandersypen et al., 2006; Yashima, 1987, 1982). Evaluating the performance of individual irrigation block only at one point in time will not adequately capture the situation within a large-scale irrigation scheme. Previously, the water balance method was conducted to evaluate the performance of the tertiary irrigation system in a relatively large-scale rice irrigation scheme (15,305 ha) in Tanjung Karang, Malaysia, which provided valuable insights into the comprehensive evaluation of water allocation for irrigation (Rowshon et al., 2014). But due to the resource-intensive requirements, the water balance model is not sustainable. In addition, the high cost of installing and maintaining measurement devices is a challenge when they are not readily available. For large-scale, multi-level irrigation systems, the limitations of the water balance method become even more apparent due to the large amount of information required and the large spatial areas that need to be covered for long-term monitoring. As a result, the approach may be less relevant and practicable in extended irrigation contexts, highlighting the need for alternative approaches that address the challenges of large spatial catchments for continuous monitoring and regular evaluation.

Quantifying irrigation water needs for large-scale rice irrigation scheme, poses a significant challenge for sustainable agriculture monitoring and other method need to explore. To reconstruct irrigation water withdrawal and irrigation water consumption data for large-scale area requires extensive modelling and input such as soil types, weather conditions and crop growth stages (Zhang et al., 2022). The limitations of conventional methods highlight the use of long-term geospatial satellite raster data in efficiently evaluate tertiary irrigation system performance across large geographical areas. The evaluation of irrigation management practices of tertiary irrigation system has been conducted based on the consumed ratio, which is the ratio of water supply to water requirement that focus on determining the amount of irrigation water needs that have been satisfied (Ragab et al., 2019; Vandersypen et al., 2006). Since secondary canals of irrigation blocks are consistently filled at designed supply quantities, determining water requirements from the rice paddy field is essential to evaluate water management of tertiary irrigation system based on good farming practices (Vandersypen et al., 2006). In the estimation of irrigation water needs, evapotranspiration (ET) is a crucial component from crop water requirement and soil water balance (Jensen et al., 1990). ET represents the water loss from soil evaporation and plant transpiration. While recent advancements have improved ET estimation with gridded data for irrigation water management, there is still a lack of consistency in soil and plant conditions across agricultural lands that requires further information that reflect the actual requirement of those information (Calera et al., 2017).

The emergence of datasets from remote sensing technology using optical-thermal satellites to measure evapotranspiration (RS-ET) has revolutionized to sustainable irrigation water management, providing a valuable tool to assess actual ET by soil and plant at a spatial scale represented by individual pixels (Bos et al., 2005; Calera et al., 2017). Satellite and airborne technologies enable broad, continuous, and near-real-time assessments across large geographic areas, particularly advantageous in regions with limited onsite data collection capabilities. However, the RS-ET that get input from satellite and processed through algorithm presents both strengths and weaknesses, influenced by various variables such as water input, soil properties, plant properties, sensible heat, etc. (Calera et al., 2017). Obtaining RS-ET can initiate difficulties due to the requirement for specialized knowledge in terminology, sensor types, data analysis, and multidisciplinary expertise (Jindo et al., 2021). Despite the ongoing debate on well-defined approach for acquiring RS-ET in irrigation system assessments, previous studies have successfully evaluated irrigation system performance using RS-ET estimates derived from various models and algorithms (Karimi et al., 2019; Poudel et al., 2021; Roerink et al., 1997; Sawadogo et al., 2020). Based on this knowledge, RS-ET has emerged as a highly advantageous tool for measuring water consumption over extensive irrigated agricultural areas (Bastiaanssen et al., 1996; Bastiaanssen and Bos, 1999; Roerink et al., 1997) and has been proposed as a parameter in a new set of irrigation performance indicators (Bos et al., 2005; Roerink et al., 1997). Several indicators exist for irrigation system evaluation, and their selection depends on the boundary conditions, as well as the purpose of the evaluation (Bastiaanssen and Bos, 1999; Bos et al., 2005). While some studies suggest that ET combined with irrigation performance indicators holds potential for evaluating irrigation systems at main, secondary and tertiary level (Ahmad et al., 2009; Kharrou et al., 2021; Roerink et al., 1997; Zwart and Leclert, 2010), a critical gap exists in understanding the applicability of RS-ET for assessing the performance of tertiary irrigation system within expansive irrigation scheme. This gap underscores the need for further investigation to clarify the method and effectiveness of remote sensing technology in tertiary irrigation system performance evaluations.

Cloud computing with Google Earth Engine (GEE) has revolutionized the way geospatial imagery is acquired and analyzed (Gorelick et al., 2017). Despite the valuable insights gained from previous studies in agriculture, hydrology, and environmental monitoring using geospatial data within the GEE platform (Elnashar et al., 2021; Laipelt et al., 2021; Zhang et al., 2019), a significant research gap persists in the regional-scale evaluation of tertiary irrigation system. This gap highlights the need for further investigation into how tertiary irrigation system in large-scale irrigation scheme are assessed using GEE. Nevertheless, numerous studies have shown that geospatial raster data from GEE can effectively monitor large-scale irrigation through parallel analysis (Deines et al., 2019, 2017; Xie et al., 2019; Zurqani et al., 2021), allowing for the seamless data collection and analysis. This approach not only enables easy analysis of surface changes but also provides a promising way to address the research gap. The interdisciplinary between water resources management, agriculture, and geospatial technology positions our study at the forefront of addressing complex challenges in large-scale irrigated systems. Consequently, this study aims to develop and implement a methodology utilizing geospatial imagery to assess tertiary irrigation system within the Muda Irrigation Scheme on a regional scale. The specific objectives include, (1) to determine rice cultivation boundary for precise data collection (2) to conduct a quantitative assessment of irrigation system performance using established irrigation performance indicators. This study aims to provide practical insights on using space data for regular evaluation of tertiary irrigation systems, enhancing efficient water management.

2. Material and methods

2.1. Description of study area and water management for rice cultivation practices

The Muda Irrigation Scheme, the largest rice granary in northern Peninsular Malaysia, supplies 45 % of the nation's rice consumption over its 126,000 ha area, with 96,500 ha dedicated to lowland rice cultivation. The operation and management of Muda Irrigation Scheme is the responsibility of the Muda Agricultural Development Authority

(MADA). The Muda Irrigation Scheme has a tropical monsoon climate, with temperatures ranging from 21 to 32 °C. Annual rainfall falls between 2032 and 2540 mm, and humidity levels in the lowlands vary from 70 % to 90 %, depending on weather conditions. For two growing seasons, rice cultivation in Muda Irrigation Scheme requires an annual irrigation water supply of 2400 mm (Rusli et al., 2022). The onset of rice planting during the main season (October–March) relies on monsoon rain, while the off-season (April–September) requires supplementary water sources. Planting dates are determined based on annual water forecasts and current environmental condition. Water sources for rice cultivation include rainfall (52 %), reservoirs (30 %), river flow (10 %), and recycled water (8 %) (Hanafiah et al., 2019; Rusli et al., 2022). Rice varieties in Muda Irrigation Scheme mature at 97–113 days, with a total growth period of four months (Fatchurrachman et al., 2022; Nazuri and Man, 2016; Rudiyanto et al., 2019). The land preparation for rice cultivation involves thorough plowing and soil saturation through flooding. Direct seeding is then carried out in flooded fields, each averaging around two hectares, situated within designated blocks ranging from 200 to 1000 ha, equipped with a secondary irrigation system. The Muda Irrigation Scheme utilizes a total of 172 irrigation blocks for rice cultivation. The topography of the area results in rice paddy fields with irregular shapes and dimensions, and within irrigation blocks, rice paddy fields are intermixed with other land uses.

This study focusing on Region II of the Muda Irrigation Scheme, the largest rice-growing region of the four regions. The authority disseminates the rice-planting schedule for managing irrigation to secondary canals in three phases for every rice-growing season. This approach enables farmers to access water and engage in rice cultivation within the designated planting window based on the specific irrigation block in which they are located. Fig. 1 shows the location of the study area and the boundary of the rice-planting schedule for the irrigation blocks. A secondary canal was used for gravity-flow irrigation during the rice cultivation period in each irrigation block. Fig. 2a shows a schematic of an irrigation block with an average infrastructure density of 10 m ha^{-1} for rice paddy fields, relying on primary and secondary canals and water control structures, such as constant head orifice (CHO) offtake, irrigation end control (IEC), and drainage end control (DEC) for water management. The main challenge arises from the low canal density (less than 10 m ha^{-1}) within the irrigation block, which leads to longer durations of water distribution during the pre-saturation period through gravitational flow from the CHO offtake to the DEC (Fujii et al., 1993). This problem is particularly pronounced for rice paddy fields situated at a distance of 1−2 kilometers from the secondary canal. Additionally, rice paddy fields located in lowland areas often have to wait for farmers in highland areas to open waterways to their plots (Baharudin and Arshad, 2015). These issues can potentially result in delays in planting and harvesting during the two consecutive growing seasons annually. To enhance the irrigation distribution and support year-round rice double cropping, authority introduced the tertiary irrigation system as depicted in Fig. 2b. This system subdivides rice paddy fields within an irrigation block into smaller irrigation service areas (ISA) by constructing tertiary-level irrigation infrastructures, including canals, drains, and farm roads, by increasing the infrastructure density to 30 m ha^{-1}. A three-stage scheduling system was initiated with the tertiary irrigation system, making use of water control structures (such as the CHO-offtake, IEC, and DEC) located along the tertiary irrigation infrastructure. Each schedule provides a 10-day window for farmers to independently withdraw water from the tertiary canal, allowing their rice paddy fields to be inundated before the next schedule. This scheduling strategy aims to complete the irrigation distribution for the block within 30 days using the tertiary irrigation system, optimizing water supply, and enabling efficient rice cultivation scheduling. Moreover, the tertiary drain

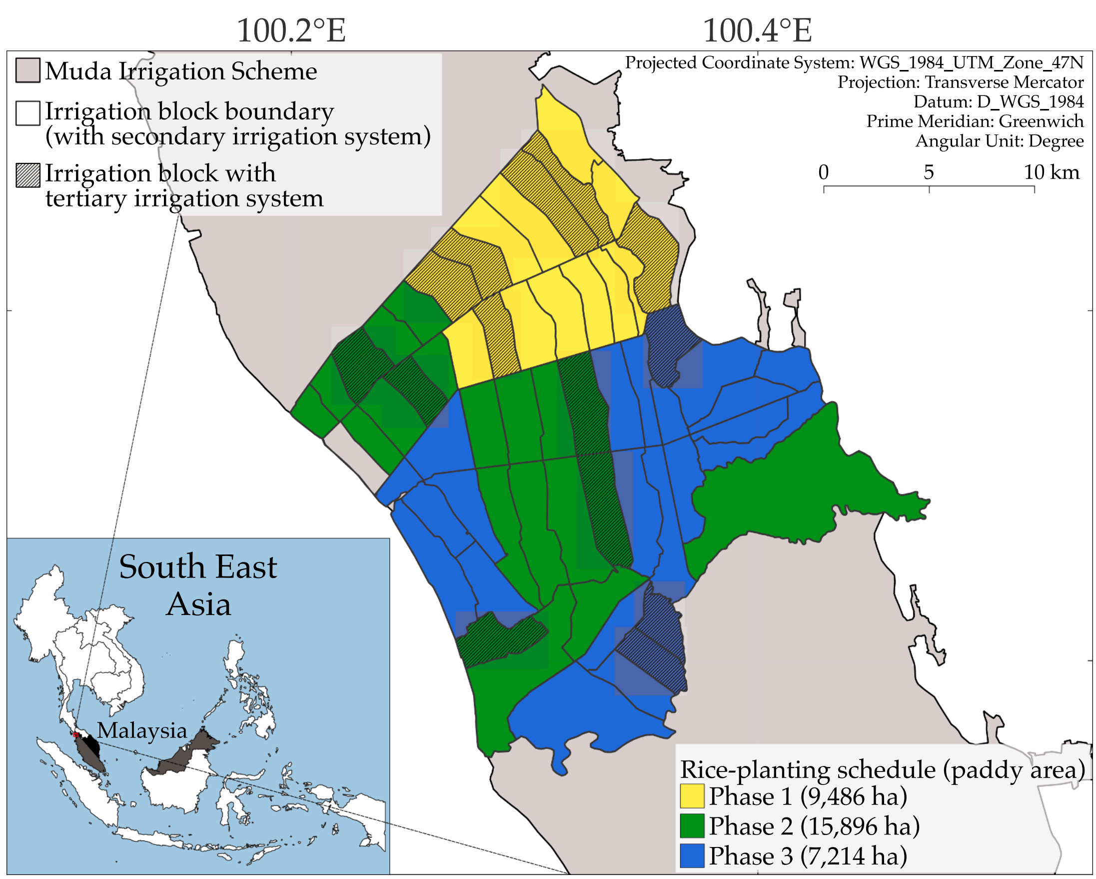

Fig. 1. The location of the study area and the boundaries of the rice-planting schedule by phase. The Region II of Muda Irrigation Scheme comprises 60 irrigation blocks, 14 of which are equipped with a tertiary irrigation system (shaded with diagonal line), while the remaining 46 are non-tertiary irrigation system.

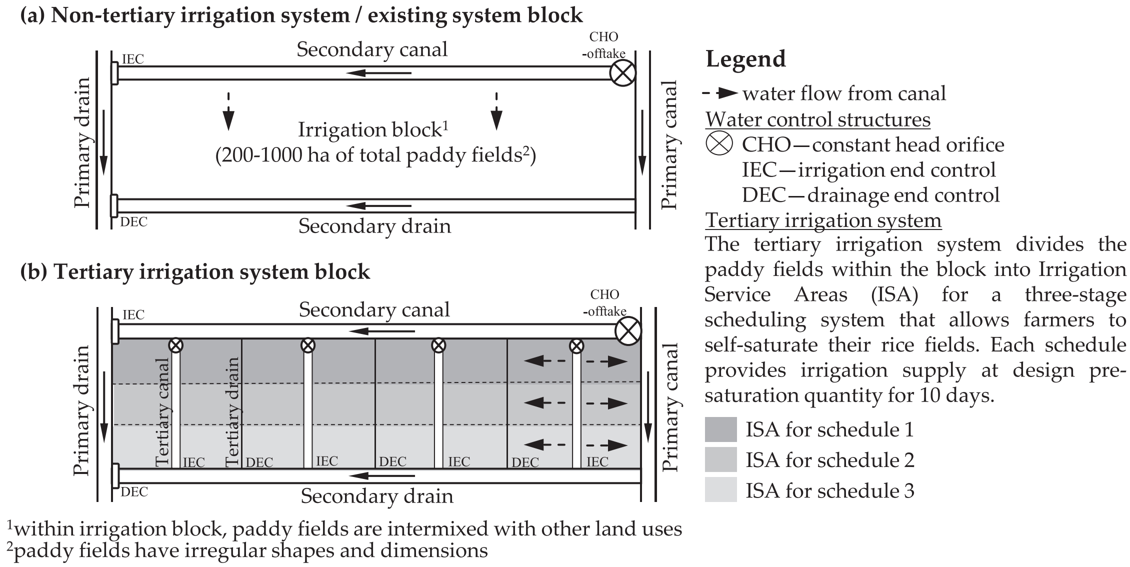

Fig. 2. Schematic facilities in an irrigation block with (a) non-tertiary irrigation system or existing system (b) tertiary irrigation system.

empowers farmers to maintain sufficient water levels in their rice paddy fields.

A previous study reported that existing systems or non-tertiary irrigation system irrigation blocks take up to 40 days to complete the pre-saturation period, whereas tertiary irrigation system can deliver water within irrigation block in less than 30 days (Fujii et al., 1993). Theoretically, with good farming practice, irrigation blocks with tertiary irrigation system should exhibit a better water distribution, thus improving the water consumption of rice plants in rice paddy fields according to schedule. However, due to financial constraints, tertiary irrigation system was selectively implemented in identified blocks facing existing irrigation and drainage challenges. As a result, irrigation blocks with tertiary irrigation system are interspersed with existing system (Fig. 1). Future plans involve expanding the development of tertiary irrigation system in all irrigation blocks, ensuring comprehensive coverage, and enhancing irrigation efficiency. Presently, of the 60 irrigation blocks in Region II, only 14 are equipped with a tertiary irrigation system built between 1980 and 2021. This number is increasing as the government aims to increase rice productivity and yield. Notably, the number of irrigation blocks with tertiary irrigation system was higher in phase 1 (6) than in phases 2 (5) and 3 (3). In terms of rice acreage, the tertiary irrigation system covers 37 % of the acreage of phase 1 (3547 ha), 18 % of the acreage of phase 2 (2848 ha) and 12 % of the acreage of phase 3 (899 ha).

2.2. Methodology

The performance of irrigation blocks with tertiary irrigation system and non-tertiary irrigation system within Region II was compared. In order to reduce the variability in rice cultivation practices resulting from the timing of water delivery to the secondary canal, the performance evaluation was conducted in monthly scale based on the rice-planting schedule provided by the authority (Table 1) over four rice-growing periods: main season 2019 (October 2018 to March 2019), off-season 2019 (April 2019 to September 2019), main season 2020 (October 2019 to March 2020), and off-season 2020 (April 2020 to September 2020). The chosen periods cover a range of environmental conditions and cropping cycles. Fig. 3 illustrates the methodological framework used in this study. Data collection and pre-processing of geospatial imagery was carried out using GEE platforms. The RS-ET served as the key metric parameter to assess the dynamics of water use within the irrigation blocks with tertiary and non-tertiary irrigation system. Since the information of rice yield was not available at block level, the Normalized Difference Vegetation Index (NDVI) was used as an additional parameter to determine yield, downscaled from locality level. A 'locality' is established by the authority to manage agricultural administration of the irrigation blocks and acted as a farmer's organization. These localities provide a wide range of services including human resource management, farmer mechanization, agricultural infrastructure, farm produce supply, financing, development and extension services, post-harvest and food processing technology, agricultural cyber resource centers and marketing (MADA, 2023). The boundaries of the localities and irrigation blocks within their management are shown in Fig. 4. Both RS-ET and NDVI were spatially acquired, pre-processed and organized to present water consumption from RS-ET and yield for individual irrigation blocks. The acquired geospatial imagery were reviewed before being used in selected irrigation performance indicators. The details of each procedure are described below.

Table 1
The date of rice-planting schedule over four rice-growing seasons. This information is used to determine the irrigation time for each block. Planting dates are determined based on annual water forecasts and current environmental conditions. The phase boundaries are shown in Fig. 1.

	Main season 2019 (October 2018 to March 2019)			**Main season 2020** (October 2019 to March 2020)		
	Phase 1	**Phase 2**	**Phase 3**	**Phase 1**	**Phase 2**	**Phase 3**
Planting start	Sep. 26	Oct. 6	Oct. 16	Sep. 25	Oct. 5	Oct. 15
Planting end	Oct. 24	Nov. 3	Nov. 13	Oct. 30	Nov. 9	Nov. 19
Irrigation end	Jan. 22	Feb. 1	Feb. 11	Jan. 28	Feb. 6	Feb. 17
	Off-season 2019 (April 2019 to September 2019)			**Off-season 2020 (April 2020 to September 2020)**		
	Phase 1	**Phase 2**	**Phase 3**	**Phase 1**	**Phase 2**	**Phase 3**
Planting start	Apr. 17	May 1	May 15	Mar. 18	Mar. 28	Apr. 7
Planting end	May 14	May 28	Jun. 11	Apr. 18	Apr. 28	May 8
Irrigation end	Aug. 13	Aug. 27	Sep. 10	N/A	N/A	N/A

N/A: Not available

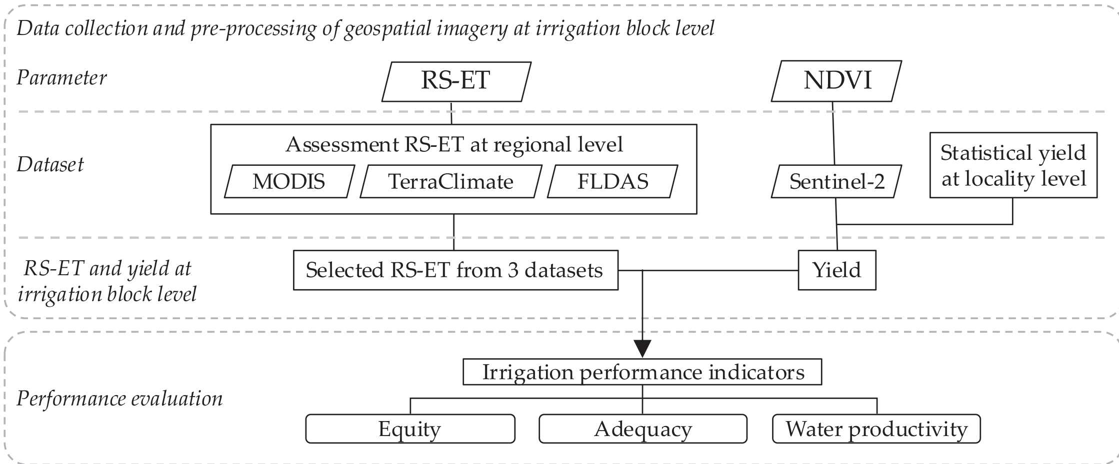

Fig. 3. Methodological framework used in this study. Data collection and pre-processing of geospatial imagery was carried out using Google Earth Engine (GEE) platforms. Remote sensing-evapotranspiration (RS-ET) and yield derived from Normalized Difference Vegetation Index (NDVI) obtained at irrigation block level was used in performance evaluation through selected indicators.

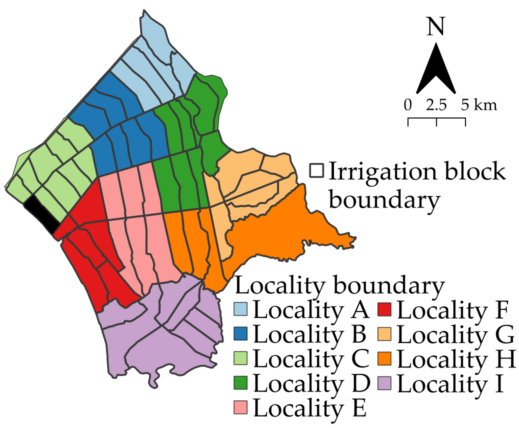

Fig. 4. The boundaries of locality and irrigation blocks. The locality coordinates agricultural management and resource utilization for irrigation blocks within their boundary. The statistical rice yield used for this study was obtained at locality level.

2.2.1. Data collection and pre-processing of geospatial imagery at irrigation block level

Region II has diverse land use. Since rice is grown year-round in the lowland rice paddy fields, the final delineation excluded all features that are not part of the rice paddy fields within the irrigation blocks in the region. These include natural dense vegetation (such as forests, rubber trees and palm trees), isolated buildings and water bodies. The focus was collecting data from large-scale irrigated rice paddy fields at recent years, where the interaction between water uses and crop productivity is significant (Conrad et al., 2020). The delineation of rice cultivation areas using optical satellite imagery is a complex task due to the varying reflectance characteristics during the different growth stages of rice. Therefore, it is important to classify land use and land cover (LULC) during the rice maturation stage. LULC classification was performed using machine learning on the GEE platform based on the successful outcomes of previous studies (Chen et al., 2020; Fatchurrachman et al., 2022; Shaharum et al., 2020).

The maturity stage of rice in January 2020 was identified as the target period for classification by machine learning with Sentinel-2. To improve the accuracy of machine learning classification in GEE, a series of image preprocessing improvements were performed for each pixel (10 × 10 m) of Sentinel-2 image. These improvements include several important steps. First, cloud masking was performed by using a filter function to identify and remove pixels with a cloud probability greater than 10 % to ensure that data obscured by cloud cover was excluded from our analysis. Next, clustering was applied to the median values of the original bands of the Sentinel-2 images to facilitate the extraction of relevant features. Relevant features include (1) additional spectral band indices such as Normalized Difference Vegetation Index (NDVI), Normalized Difference Water Index (NDWI), Modified Normalized Difference Water Index (MNDWI), and Normalized Difference Built-Up Index (NDBI) to characterize rice in paddy fields, open water areas, and urban areas (McFeeters, 1996; Xu, 2006; Zha et al., 2003); (2) topographic features (Franklin, 1995) to detect lowland areas; and (3) a normalized algorithm to reduce band value variations and fluctuations (Zhao et al., 2020). The categorization of each pixel was carried out using a random forest classifier, where the features were obtained from specified reference points (Rodriguez-Galiano et al., 2012; Shaharum et al., 2020; Shetty et al., 2021). Additionally, supplementary datasets including Google Street View were incorporated during the process of sampling reference points. The accuracy assessment was computed by confusion matrix as demonstrated in studies involved machine learning classification (Basheer et al., 2022; Feizizadeh et al., 2023). Validation of rice cultivation areas after machine learning classification process relied on knowledge of feature locations, visual inspection of recent composite images, and statistical records from relevant authorities. The final step was to convert the classified rice paddy field raster into a vector polygon (GEE, 2022). This polygon represents the rice cultivation areas within the study area and was used to collect the required parameters.

The first parameter collected was RS-ET, from three global RS-ET datasets within GEE: MODIS, TerraClimate, and FLDAS. The first dataset, MODIS-ET (Dataset: MODIS/061/MOD16A2GF), has a 0.5 km resolution and offers eight-day cumulative actual ET water loss totals in mm. RS-ET from MODIS-ET was derived from the MOD16 ET al.gorithm using the Moderate Resolution Imaging Spectroradiometer (MODIS) satellite sensor. More detailed explanations of MOD16 ET can be found in Mu et al. (2007). RS-ET of MODIS-ET was organized on a monthly scale to represent the growth of rice plants in the target period. The MOD16 ET al.gorithm considers evaporation from the soil, wet canopy, and transpiration of the vegetation both during the day and at night. The updated MOD16 ET al.gorithm, which has evolved since the 2010 dataset, was cross-validated with an eddy flux tower in the United States (Mu et al., 2011). Confirmation for the use of MODIS-ET in our study area was also based on the recent validation of seven global RS-ET values in Thailand (Sriwongsitanon et al., 2020). Sriwongsitanon et al. (2020) indicate that MODIS-ET showed the most promising results for tropical environmental conditions similar to our study area compared to the other datasets. Potential evapotranspiration (PET) represents the maximum ET that can be achieved at a specific location and under specific environmental conditions. The RS-PET time series was similarly extracted from the MODIS-ET dataset in the GEE as a separate layer. Both the RS-ET and RS-PET parameters in MODIS-ET were calculated using the energy balance and Penman-Monteith algorithm and underwent gap filling from contaminated clouds and/or aerosols according to the latest version of the dataset's user manual (Running et al., 2021). Given the insufficiency of high-resolution global RS-ET data, a comparison was made between MODIS-ET monthly RS-ET and TerraClimate-ET (~4 km resolution) (Dataset: IDAHO_EPSCOR/TERRACLIMATE) (Abatzoglou et al., 2018) as well as FLDAS-ET (~10 km resolution) (Dataset: NASA/FLDAS/NOAH01/C/GL/M/V001) (McNally et al., 2017). Both datasets present actual ET as a monthly total water loss in millimeters, derived from different models using climate and meteorological data from remote sensing technology (Abatzoglou et al., 2018; McNally et al., 2017). The availability and applicability of the RS-ET obtained from GEE was assessed based on number of pixels, temporal pattern, and recorded value for four rice-growing periods on a monthly scale.

The second parameter collected was NDVI. Since the block-level yields were unavailable, NDVI was used to estimate them by aggregating pixel yields within the blocks. Yield determination at the pixel level involved downscaling higher-level yield statistics using NDVI through linear regression (Cai and Sharma, 2010; Poudel et al., 2021; Shirsath et al., 2020). The NDVI was primarily used to detect the presence of chlorophyll in plants, which is crucial for interpreting vegetation dynamics based on rice plant phenology (Zheng et al., 2016). The NDVI value is a unitless metric and reflects higher green vegetation intensity as it approaches 1. The NDVI used in this study was obtained from the Sentinel-2 satellite (10 m resolution) (Dataset: COPERNICUS/S2_SR). To determine the NDVI from Sentinel-2, the red (band 4) and near infrared (NIR) (band 8) reflectance measurements were used to capture the green reflectance. Each pixel in the Sentinel-2 images was subjected to a filtering process to ensure that the probability of clouds and shadows occurring was less than 5 %. In this study, the ratio of the one-pixel yield was downscaled from locality level and subsequently aggregated into block boundaries. The boundaries of irrigation blocks and their localities, as well as the yield statistics, were obtained from the authority and then imported into the GEE user assets for data management and verification in obtaining the processed satellite data. The process of yield determination is shown in Eqs. (1)–(4), where F is the weighting factor and is the ratio of the one-pixel NDVI to the total value of NDVI over all pixels (n) in the locality based on the maximum NDVI values for each growing season. Y is the statistical yield in kilogram (kg) at locality level for each season and A is the area of one pixel of Sentinel-2 imagery (10 m × 10 m). However, the validation process of yield at block level was restricted by the availability of ground data. Since individual pixel-wise yield values were downscaled from high-quality statistical data and aggregated, these aggregated values were then compared to the officially reported figures (Cai and Sharma, 2010; Poudel et al., 2021; Shirsath et al., 2020)

$$\mathrm{Yield_{irrigation\ block}} = \sum \mathrm{Yield_{pixel}\,within\ irrigation\ block,\ unit\ in\ kg} \tag{1}$$

$$\mathrm{Yield_{pixel}} = \frac{\mathrm{F} \times \mathrm{Y_{locality}}}{\mathrm{A_{pixel}}} \tag{2}$$

$$\mathrm{F} = \frac{\mathrm{NDVI_{pixel}}}{\mathrm{NDVI_{locality}}} \text{ , where} \tag{3}$$

$$\mathrm{NDVI_{locality}} = \sum_{i=1}^{i=n} \mathrm{NDVI_{pixel}} \tag{4}$$

Additional information such as monthly rainfall data was obtained from the Alor Star meteorological radar station (6.1248° N, 100.3678° E) to verify weather conditions during the study period. The station is located in the center of Region II of the Muda Irrigation Scheme provided by the Malaysian Meteorological Department (MMD).

2.2.2. Performance indicators

The concept of irrigation system performance is broad and there is no single solution has been discovered to address it. Performance indicators provide a means to evaluate irrigation systems from various perspectives, allowing the measurement of their efficiency and sustainability (Elshaikh et al., 2018). Recent advances in satellite-measured parameters and established remote sensing-based performance indicators have provided valuable tools for irrigation system evaluation (Akhtar et al., 2018; Poudel et al., 2021; Sawadogo et al., 2020; Usman et al., 2014). However, exploration of this approach for tertiary-level irrigation systems located within a large-scale irrigation system has not yet been conducted. This study focused on the evaluation of tertiary and non-tertiary irrigation system irrigation blocks in large-scale areas. The evaluation was conducted separately according to the three-phase rice-planting schedule established by the authority (see Table 1 and the boundary shown in Fig. 1) to account for the variability of agricultural practices due to rice planting timing. Assuming that each phase is supplied with water at the same time, the utilization of the tertiary and non-tertiary irrigation systems should be comparable with respect to the monthly scale. Therefore, the water consumption and yield for the respective irrigation blocks were used in the irrigation performance indicators as explained below.

The first indicator is equity which measures distribution of fair amount within irrigation system. Sawadogo et al. (2020) employed an equity indicator to assess water consumption uniformity among three crop types: rice, maize, and sweet potatoes by determined the ET variability for each crop through coefficient of variation (CV). Similarly, Roerink et al. (1997) evaluated the equity of two irrigation systems by analyzing CV of ET in each system. This study builds upon previous research by comparing the CV of RS-ET between tertiary and non-tertiary irrigation systems blocks that satisfied the water supply of farming management using equity indicator. The equity is calculated from Eqs. (5) and (6). A system with higher CV indicated greater variability in water loss from RS-ET within the irrigation system, leading to less uniform water consumption across the irrigation block. According to Bastiaanssen et al. (1996), achieving good uniformity in crop water consumption is linked to equitable irrigation water distribution, characterized by a CV of less than 10 %.

$$\mathrm{CV}(\%) = \frac{\mathrm{SD}}{\bar{x}} \times 100\% \text{ , where} \tag{5}$$

$$\mathrm{SD} = \sqrt{\frac{1}{n}\sum_{i=1}^{i=n} |x_i - \bar{x}|^2} \tag{6}$$

where	SD	=	standard deviation
	i	=	irrigation block
	n	=	total number of irrigation block in the irrigation system
	x_i	=	RS-ET of irrigation block (mm)
	$\bar{x}$	=	average value of the RS-ET of all irrigation blocks within the irrigation system (mm)

The second indicator is adequacy which measures distribution of required amount within irrigation system. An adequacy indicator offers insights into the well-watered croplands. Relative evapotranspiration (RET) (unitless), calculated as the ratio of RS-ET to RS-PET, as shown in Eq. (7), can serve as an effective means of evaluating the adequacy of irrigation systems (Kharrou et al., 2013; Sawadogo et al., 2020). In this study, the RS-ET and RS-PET values obtained for each irrigation block were used to calculate the RET and assess the adequacy of both tertiary and non-tertiary irrigation systems. An adequacy value of 0.75, as established by Roerink et al. (1997), is considered to be the accepted reference point for irrigation system performance.

$$\text{RET (unitless)} = \frac{\text{RS} - \text{ET}_{\text{irrigation block}}}{\text{RS} - \text{PET}_{\text{irrigation block}}} \tag{7}$$

The third indicator is water productivity which assesses the yield on average water consumption. Water productivity indicator measures the efficiency of irrigation systems through crop water productivity (CWP) (unit: kg m^{-3}) (Blatchford et al., 2019; Poudel et al., 2021; Sawadogo et al., 2020). Alberto et al. (2011) employed this indicator in a case study comparing water productivity between two irrigation techniques: flooded and aerobic soil conditions. CWP is calculated by determining the ratio of crop yield for each irrigation block to the accumulated RS-ET from the start of the season (SOS) to the end of the season (EOS) in the irrigation block (Zwart and Bastiaanssen, 2004). The CV of CWP (unit: percentage (%)) was used for comparison; a low percentage indicates good water productivity by consistency from CV values, while a high percentage suggests the need for improved water management (Zwart and Bastiaanssen, 2007).

$$\text{CWP}(\text{kg m}^{-3}) = \frac{\text{Yield}_{\text{irrigation block}}}{\sum_{\text{SOS}}^{\text{EOS}} \text{RS} - \text{ET}_{\text{irrigation block}}} \tag{8}$$

$$\text{Water productivity of irrigation system (\%)} = \text{CV of CWP} \tag{9}$$

3. Results

3.1. Applicability of GEE to obtain geospatial data

3.1.1. Rice cultivation areas generated from machine learning

The machine learning classification was used to generate vector polygon of rice cultivation areas at regional scale from composite satellite image at recent years. From this process, rice paddy fields accounted for the largest area at 77 % of whole region, followed by urban at 11 %, non-rice vegetation at 6 % (including forests, rubber trees, palm trees, and others) and water bodies at 6 %. The processes for extracting the boundaries for the rice paddy fields is illustrated in Fig. 5. The output of the classified pixels of the four different land use classes is shown in Fig. 5a, followed by the visual inspection of rice paddy fields vector polygon from high definition satellite image (Fig. 5b) and final extracted rice paddy fields within individual irrigation blocks (Fig. 5c). The accuracy assessment of this proses represented by a confusion matrix is shown in Table 2. Based on the results, final classified raster of the four distinct land uses in Region II had an overall accuracy of 83.4 % and a kappa coefficient of 0.78. The producer's accuracy for rice paddy fields was 84.4 % indicating the process effectively classified 84.4 % of the particular land uses. However, the user's accuracy was 78.4 %, suggesting a slightly lowered prediction accuracy for this particular land use. Nevertheless, despite the similar color characteristics of green vegetation between rice and non-rice in the optical raster data, the user's accuracy for non-rice is higher at 95.2 % and the extraction processes (Figs. 5a–5c) clearly show the distinctness for both land use classes. Furthermore, the rice paddy fields areas that derived from the satellite imagery (31,486 ha), matched the most recent authority statistics at the regional scale (32,595 ha), with a relatively small difference of 3.5 %,

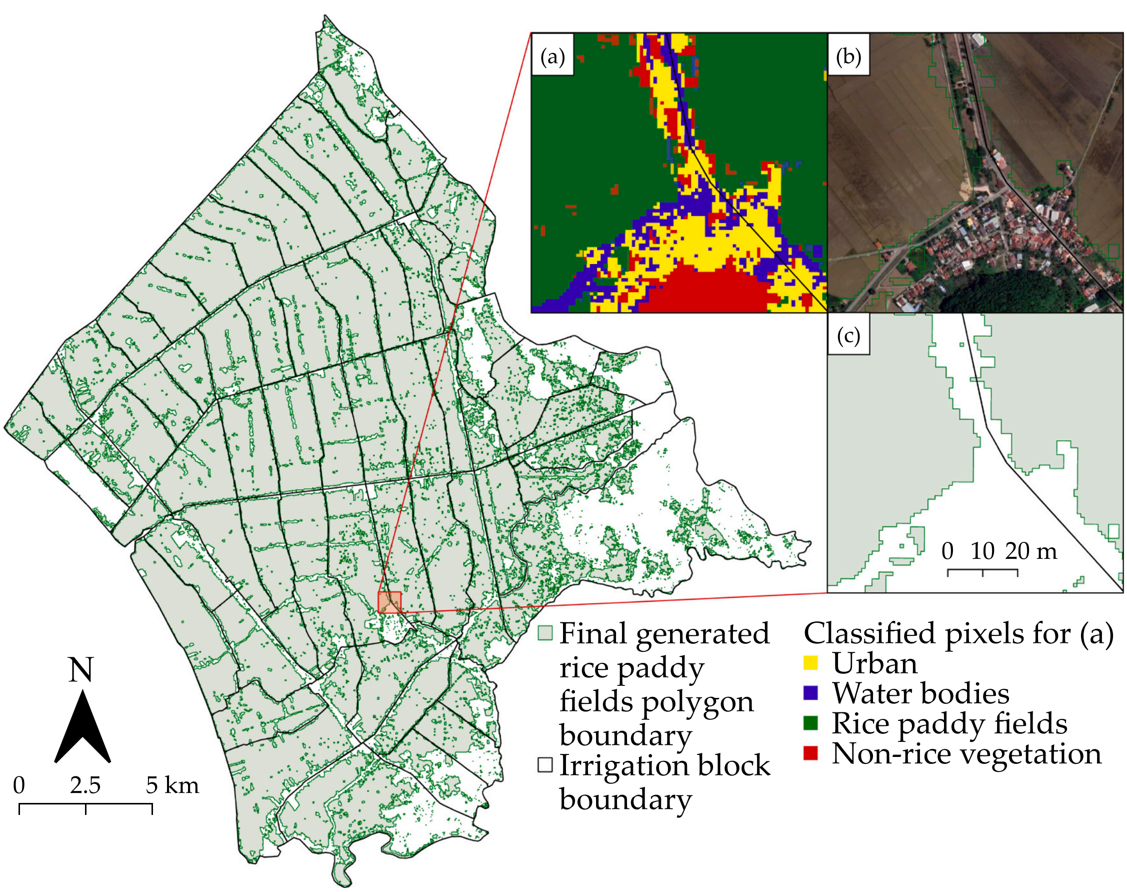

Fig. 5. Boundary extraction process for rice cultivation areas in irrigation blocks derived from optical satellite imagery. (a) Classified pixels of four types of land use, (b) Visual inspection of rice paddy fields vector polygon with high definition satellite image, (c) Extracted rice paddy fields polygon in each irrigation block.

Table 2
Confusion matrix for the machine learning classification.

		Reference data					
		Urban	Water bodies	Rice paddy fields	Non-rice vegetation	Total	User's Accuracy
Classified data	Urban	66	8	2	0	76	80.5 %
	Water bodies	7	66	8	1	82	83.5 %
	Rice paddy fields	7	5	76	2	90	78.4 %
	Non-rice vegetation	2	0	11	59	72	95.2 %
	Total	82	79	97	62	320	
	Producer's accuracy	86.8 %	80.5 %	84.4 %	81.9 %		
	Overall accuracy	83.4 %					
	Kappa	0.78					

ranging from 6 % to 24 % at the locality scale. The delineation of a target area for crop intensity allows a more comprehensive assessment of irrigation efficiency (Bos et al., 1994). Therefore, rice paddy fields boundary was extracted from the classified raster using masking function was applied to create a vector polygon. This polygon was used to collect geospatial data.

3.1.2. Data acquisitions over target periods

The average RS-ET data obtained from MODIS, TerraClimate, and FLDAS datasets for Region II of the Muda Irrigation Scheme are shown in Table 3. Since ground ET measurement is difficult due to the high cost of equipment installation in large-scale areas, RS-ET datasets were verified by three assessment approaches.

The first assessment of RS-ET is based on the total pixels. MODIS-ET reports the highest count at 1276, while Terraclimate-ET records 24 and FLDAS-ET comes in at 5 with good coverage ranging from 96 % to 100 %. Despite FLDAS-ET and TerraClimate-ET achieving a 100 % and 96 % coverage rate respectively, their spatial resolution of 10 × 10 km and 4 × 4 km limits their ability to capture variations at the irrigation block level. Compared to MODIS-ET, a higher percentage of pixel counts (98 %) is achievable for the entire rice-growing area at a high spatial resolution of 0.5 × 0.5 km. This high resolution allows for precise agricultural water consumption representation from RS-ET at the irrigation block level.

The second assessment was based on monthly temporal patterns. In traditional rice irrigation practices, standing water in rice paddy fields is usually drained when rice plants approach maturity to support root growth and grain retention (Thakur et al., 2018). Consequently, ET rates decrease when the field is no longer irrigated (Roerink et al., 1997). This information supported the identification of the critical irrigation period used in this study. The results showed that the irrigation period spanned four months from land preparation to rice plant maturation, which was consistent with the authority schedules and the total growth period of rice varieties in the Muda Irrigation Scheme. In particular, this pattern was consistent with MODIS-ET compared to TerraClimate-ET and FLDAS-ET in representing the rice plant growth and irrigation period for each growing season.

The third assessment was conducted based on the recorded RS-ET values. The recorded seasonal average values of MODIS-ET, TerraClimate-ET, and FLDAS-ET were 501, 640, and 740 mm respectively, with higher values in the off-season. These values are consistent with the common ET for rice, which ranges from 400–800 mm depending on environmental conditions (Zwart and Bastiaanssen, 2004). Previous studies reported cumulative ET values for the entire rice growing season in the Muda Irrigation Scheme estimated between March and September, which amounted to 840 mm (Cabangon et al., 2002), with an annual range of 1360–1490 mm (Tukimat et al., 2012). Notably, the ET values reported by Cabangon et al. (2002) and Tukimat et al. (2012) were higher than the RS-ET values obtained in this study. Further investigation revealed that the annual rainfall values recorded during the target period tended to be higher (11–20 %) than those reported in previous studies. This is consistent with the findings of Tukimat et al. (2017), concluded that increased rainfall could reduce water loss through ET values for tropical rice fields.

Based on these assessments, particularly the first, MODIS-ET was identified as the most suitable choice for determining variation at block level, outperforming TerraClimate-ET and FLDAS-ET. RS-ET from MODIS was then arranged according to irrigation block.

The range distribution of from selected RS-ET dataset and yield of 60 irrigation blocks are shown in Table 4. Yield varied from ±0.1 and ±0.3 at the irrigation block level, scaled down from the locality level. The RS-ET at the irrigation block level showed a similar pattern to the average RS-ET at the regional level (Table 3). The approach demonstrates parallel data collection at the regional and irrigation block levels across multiple rice-growing seasons through cloud computation. With this approach, we can analyze the performance indicators more efficiently.

3.2. Performance evaluation of tertiary irrigation system

The evaluation compares the performance of the tertiary and non-tertiary irrigation systems within Region II based on the rice-planting schedule for four consecutive rice-growing seasons. The performance of the irrigation system in terms of equity and adequacy indicators is shown in Fig. 6 and Fig. 7, respectively, which were conducted based on the irrigation period. Fig. 8 shows the performance of the irrigation system based on water productivity, which was carried out on a seasonal basis.

Bastiaanssen et al. (1996) identified a CV of less than 10 % as an indicator uniform water consumption from equitable distribution of irrigation water. As shown in Fig. 6, both the tertiary and non-tertiary irrigation systems generally showed satisfactory equity as they were below the threshold. However, the tertiary irrigation system showed a remarkable performance during the irrigation period in the off-season, by consistently falling below the acceptable threshold (2−8 %) in all phases. Notably, the tertiary irrigation system in phase 1 consistently outperformed the others (3–10 %) across all growing seasons (Fig. 6a), followed by phase 2 (2–11 %) and phase 3 (2–13 %) (Fig. 6b and Fig. 6c, respectively).

In terms of adequacy, the performances of tertiary and non-tertiary irrigation systems were similar during the irrigation period, as shown in Fig. 7a−7c. However, the tendency to reach an acceptable threshold (0.75) was higher in the third month of the irrigation period for all phases (0.63−0.82), except for the tertiary irrigation system scheduled in phase 3 in the main season 2020 (0.43−0.54). Throughout the study period, the tertiary irrigation system in phase 1 showed better adequacy performance (median: 0.67, maximum: 0.82) than phase 2 (median: 0.64, maximum: 0.80) and phase 3 (median: 0.60, maximum: 0.64).

CWP focuses specifically on the evaluation of crop yield per unit of water consumed (Zwart and Bastiaanssen, 2004). In this study, CWP was determined at the irrigation block level based on downscaled crop yields and seasonal water losses through RS-ET in four consecutive growing seasons. Cabangon et al. (2002) reported that the CWP for direct seeding practice at relatively smaller scale (30−54 ha) during off-season in the Muda Irrigation Scheme ranges from 0.48−0.54 kg m^{-3}. However, with our approach, CWP values at the irrigation block scale tended to be higher (0.90−1.45 kg m^{-3}) with an average of 1.16 kg m^{-3}. Over the

Table 3
Data acquisition of average remote sensing-evapotranspiration (RS-ET) obtained in Region II using Google Earth Engine (GEE).

	Rainfall (mm)	Pixels count and coverage percentage			RS-ET value (mm)				Rainfall (mm)	Pixels count and coverage percentage			RS-ET value (mm)		
		MODIS[a] (1276)	TerraClimate[b] (24)	FLDAS[c] (5)	MODIS	TerraClimate	FLDAS			MODIS[a] (1276)	TerraClimate[b] (24)	FLDAS[c] (5)	MODIS	TerraClimate	FLDAS
Main season 2019 (October 2018 to March 2019)								**Main season 2020** (October 2019 to March 2020)							
*Oct.	267.4	98 %	96 %	100 %	72.3	106.6	120.1	*Oct.	508.8	98 %	96 %	100 %	60.4	114.8	139.3
*Nov.	149.6	98 %	96 %	100 %	95.8	99.3	123.9	*Nov.	140.8	98 %	96 %	100 %	85.7	107.4	137.8
*Dec.	189.2	98 %	96 %	100 %	99.3	105.1	132.5	*Dec.	10.4	98 %	96 %	100 %	107.2	96.4	169.0
*Jan.	62.6	98 %	96 %	100 %	116.7	106.2	162.8	*Jan.	1.4	98 %	96 %	100 %	140.7	76.0	123.5
Feb.	106.6	98 %	96 %	100 %	43.8	87.6	118.8	Feb.	44.0	98 %	96 %	100 %	66.3	46.7	83.7
Mar.	44.4	98 %	96 %	100 %	40.6	108.0	87.7	Mar.	56.4	98 %	96 %	100 %	32.4	60.4	71.2
Off-season 2019 (April 2019 to September 2019)								**Off-season 2020** (April 2020 to September 2020)							
Apr.	273.6	98 %	96 %	100 %	40.7	122.1	116.3	*Apr.	253.8	98 %	96 %	100 %	61.0	140.2	113.6
*May.	245.4	98 %	96 %	100 %	86.8	128.1	132.4	*May.	249.0	98 %	96 %	100 %	57.7	119.8	98.2
*Jun.	199.6	98 %	96 %	100 %	89.2	115.8	133.6	*Jun.	121.0	98 %	96 %	100 %	92.3	113.3	124.3
*Jul.	227.2	98 %	96 %	100 %	102.2	127.5	126.3	*Jul.	377.8	98 %	96 %	100 %	112.5	117.2	129.4
*Aug.	257.8	98 %	96 %	100 %	101.1	122.5	132.8	Aug.	141.2	98 %	96 %	100 %	109.8	124.7	136.8
Sep.	104.4	98 %	96 %	100 %	86.0	110.9	122.9	Sep.	328.8	98 %	96 %	100 %	103.4	10.4	127.7

* Irrigation duration for rice cultivation based on the authority schedules (Table 1), rounded to the month with the most days
[a] MODIS has coverage of 0.5 × 0.5 km for one pixel. Total pixels of MODIS-ET in Region II are 1276
[b] TerraClimate has coverage of 4 x 4 km for one pixel. Total pixels of TerraClimate-ET in Region II are 24
[c] FLDAS has coverage of 10 x 10 km for one pixel. Total pixels of FLDAS-ET in Region II are 5

past 20 years, the higher CWP may be attributed to the increase in relatively high yields, which are 1–2 t ha^{-1} higher than those previously reported (Cabangon et al., 2002). Notably, obtained CWP varied according to environmental conditions and were generally higher in the main season. The values were consistent with the global CWP range (0.4–1.6 kg m^{-3}) for rice reported by Zwart and Bastiaanssen (2004). The statistical distribution of CWP between the tertiary and non-tertiary irrigation systems is shown in Table 5.

In the evaluation of water productivity, a comparison of the CV of CWP between tertiary and non-tertiary irrigation systems is shown in Fig. 8. A low percentage in irrigation systems indicates favorable water productivity, while a high percentage indicates the potential for improved water management practices (Zwart and Bastiaanssen, 2007). Despite notable weather fluctuations during the main season rice growing period, tertiary irrigation system consistently had better performance than non-tertiary irrigation system, as evidenced by consistently lower percentage values. This trend is particularly pronounced in the main season of 2019, with the percentage difference in water productivity between tertiary and non-tertiary irrigation systems ranging from 0–4 %. Overall, the tertiary irrigation system achieved robust water productivity across all phases (Fig. 8a–8c). On closer examination, the tertiary irrigation system shows moderate performance in the off-season 2019 and main season 2020 (both with a magnitude difference ranging between 1–3 %), and comparatively lower in the off-season 2020 (difference of magnitude ranging between 2–4 %). A higher percentage difference in magnitude between irrigation systems indicates a significant discrepancy in the relative variability of water productivity. In contrast, smaller magnitudes indicate greater similarity in water productivity between the two systems. The variation of water productivity in all phases rice-planting schedule across rice-growing seasons highlights the need for periodic monitoring and regular evaluation.

In summary, the results indicate that the tertiary irrigation system largely met its primary objectives in terms of uniform water consumption, maintaining adequate water levels in the field, and optimizing yields per unit of water consumption, especially in phase 1. In particular, the tertiary irrigation system served a higher rice acreage in phase 1 (37 % of 3547 ha), suggesting higher performance compared to phase 2 and phase 3.

4. Discussion

4.1. Sustainability of tertiary irrigation system evaluation in large-scale irrigation scheme

A solution to provide continuous monitoring data and regular evaluation for tertiary irrigation system in large-scale irrigation scheme was demonstrated in this study. Previous studies evaluating tertiary irrigation system in the study area had found a potential water savings of 22 % (Fujii et al., 1993) and a 20 % increase in the efficiency of irrigation supply to the field for agricultural activities during the off-season growing period (Kitamura, 1988). Although our approach did not provide quantitative data on irrigation supply as shown by previous studies, our approach was able to capture the functionality of the tertiary irrigation system from three irrigation performance indicators using average gridded water use. In line with Kitamura (1988), who emphasizes the efficiency of irrigation supply in the off-season of rice-growing period, our study showed that this supply leads to uniform water consumption within the irrigation block during the same period. Compared to the non-tertiary irrigation system, the equity indicator shows that the tertiary irrigation system is consistently below the threshold (10 %), which in between 2–8 % during the off-season (Fig. 6). The adequacy indicator did not show any significant performance of the tertiary irrigation system and had relatively moderate performance (Fig. 7). Nevertheless, the monthly fluctuations of both equity and adequacy indicators highlight the need for regular evaluation of the tertiary

Table 4
The range distribution of yield and remote sensing-evapotranspiration (RS-ET) obtained for 60 irrigation blocks.

	Main season 2019 (October 2018 to March 2019)		**Off-season 2019** (April 2019 to September 2019)		**Main season 2020** (October 2019 to March 2020)		**Off-season 2020** (April 2020 to September 2020)	
Yield per locality (t ha^{-1})	5.3 ± 0.5		5.9 ± 0.3		6.1 ± 0.5		6.0 ± 0.6	
Yield per irrigation block (t ha^{-1})	5.3 ± 0.6		5.9 ± 0.6		6.1 ± 0.6		6.0 ± 0.8	
Range RS-ET per irrigation block (mm)	*Oct.	:62–83	Apr.	:35–45	*Oct.	:52–68	*Apr.	:35–69
	*Nov.	:81–118	*May.	:84–92	*Nov.	:75–98	*May.	:53–65
	*Dec.	:72–127	*Jun.	:80–101	*Dec.	:64–143	*Jun.	:81–111
	*Jan.	:75–144	*Jul.	:77–133	*Jan.	:70–164	*Jul.	:90–139
	Feb.	:28–94	*Aug.	:80–117	Feb.	:42–112	Aug.	:83–135
	Mar.	:36–52	Sep.	:85–96	Mar.	:30–50	Sep.	:82–127

* Irrigation duration for rice cultivation based on the authority schedules (Table 1), rounded to the month with the most days

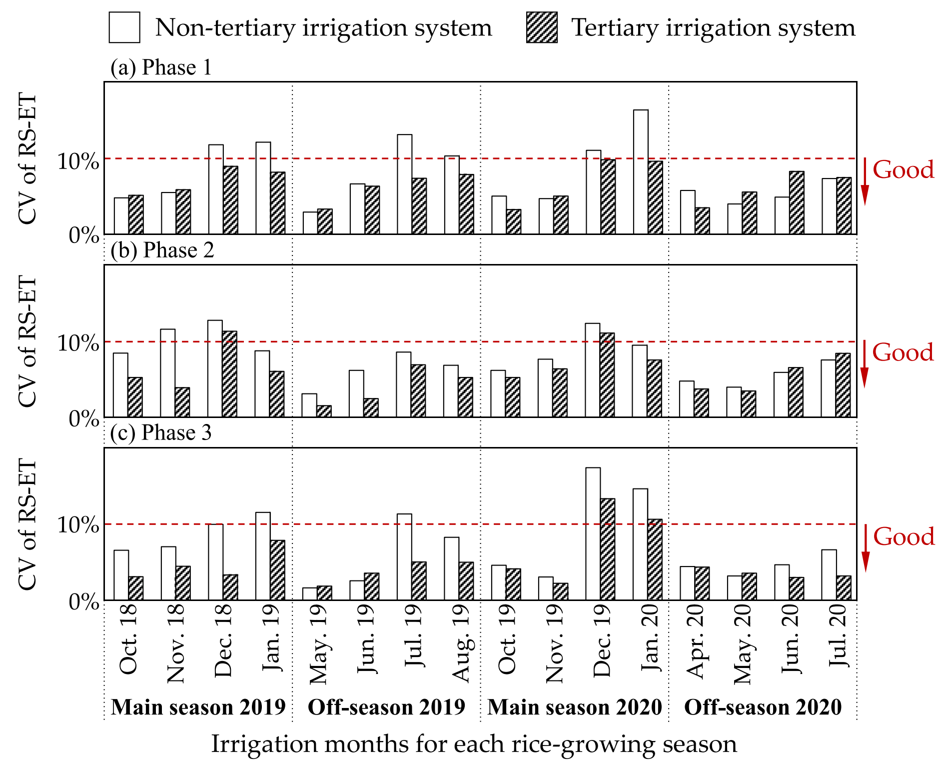

Fig. 6. Equity evaluation based on rice-planting schedule (a) Phase 1 (b) Phase 2 (c) Phase 3. The threshold of good irrigation system performance is indicated by the red dotted lines (Coefficient of variation of RS-ET less than 10 %).

irrigation system in clarifying the distribution of irrigation and water consumption under different weather conditions since rainfall is the main source of rice cultivation in this area. Sudden weather changes were observed during main seasons, particularly in the year of 2020. The sharp drop in rainfall (Table 3) and the measures taken by the authorities to support the water supply from other sources were observed during this particular rice growing season (Malaymail, 2020; Sekaran, 2020). Although the rice growing season starts with high rainfall in the main season and water was efficiently distributed during the irrigation period (based on the equity and adequacy indicators), sudden weather changes towards the time of rice harvest affected the seasonal evaluation. Reduced water supply leads to drier soils. Even though no information on the amount of additional water to support rice plant growth provided in this study, there was evidence that sudden changes in weather affected seasonal RS-ET values for rice plants. In particular, MODIS-ET showed a sudden decrease, especially after the irrigation period in February and March (Table 3 and Table 4). This situation was of particular concern if the system did not distribute the additional water sources as expected. Therefore, continuous monitoring and regular evaluation are one of the solutions to identify parts of the system that are not effective and to take further countermeasures. For example, this study also evaluated the effectiveness of the tertiary irrigation system based on current water management strategy, which divides the cultivation timing and water distribution into three phases, revealing noticeable operational variations between the tertiary irrigation system at different phases. In particular, the tertiary irrigation system serving in the rice-growing areas of phase 1 showed higher efficiency compared to the systems in the other phases (Fig. 6–Fig. 8). Given the observed variations in all indicators influenced by weather conditions, the results highlight the importance of conducting assessments in each rice-growing season to improve the overall efficiency of the tertiary irrigation system in large-scale irrigation scheme for the following seasons.

This study focused on gathering information and evaluating tertiary irrigation system across a wide area that can be used by authority to identify areas of good and poor performance of the tertiary irrigation system in the study regions. Previous evaluations of the tertiary irrigation system in the study region relied on the water balance method, which is crucial for monitoring resource sustainability and crop yield productivity in individual irrigation blocks (Fujii et al., 1993; Kitamura,

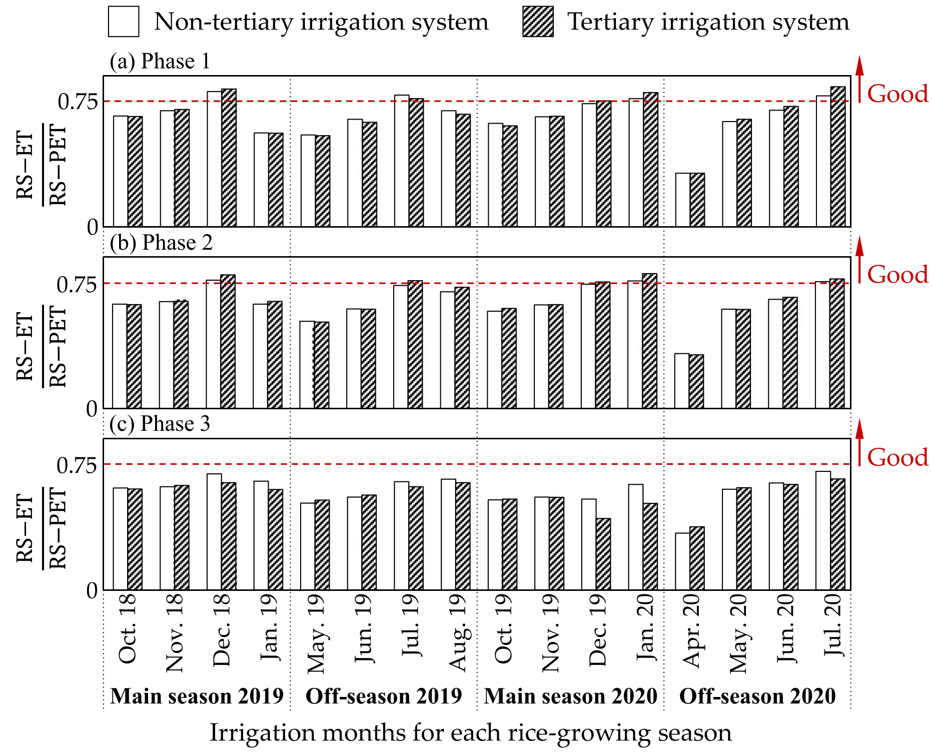

Fig. 7. Adequacy evaluation based on rice-planting schedule (a) Phase 1 (b) Phase 2 (c) Phase 3. The threshold of good irrigation system performance is indicated by the red dotted lines (Ratio of RS-ET to the RS-PET more than 0.75).

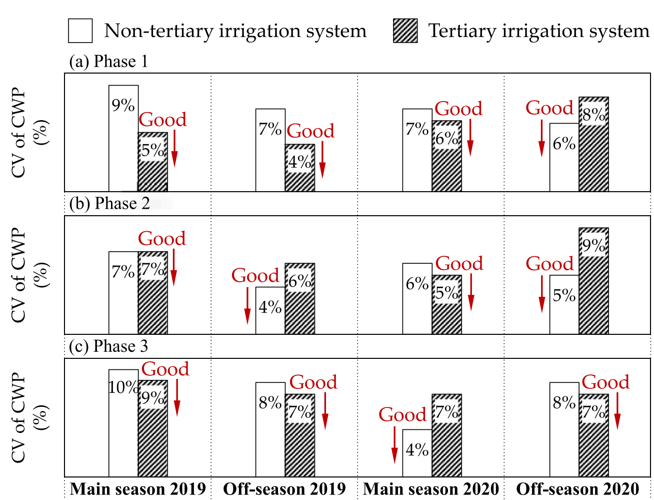

Fig. 8. Water productivity evaluation based on rice-planting schedule (a) Phase 1 (b) Phase 2 (c) Phase 3. A low percentage indicates good water productivity, while a high percentage suggests the need for improved water management for the irrigation system.

1988). However, assessment of the entire irrigation scheme is equally important for the improvement of water management strategy. With our method, recent rice cultivation areas were generated to provide seamless data collection, and a prompt assessment can be conducted, enabling a quick understanding of the current situation. Over the past 30 years, tertiary irrigation system evaluation of the Muda Irrigation Scheme has not been available because of the resource-intensive nature of direct measurements and water balance calculations at multiple levels. The GEE not only facilitates geospatial analysis for extracting rice fields in large-scale irrigation schemes (Fig. 5) but also enables access and spatiotemporal management geospatial data at the irrigation block scale (refer to Table 4). This capability allows for a rapid and cost-effective analysis. Users can conveniently download the final output of the processed data in a comma-separated value (CSV) file that is compatible with various software applications. Utilizing open-source remote sensing datasets for monitoring and evaluating irrigation system performance is essential, as it proves to be a cost-effective and efficient analysis method, especially when in-situ data are challenging to obtain (Zwart and Leclert, 2010). The applicability of our method to other regions worldwide depends on prerequisites such as availability on statistical information of rice yield and rice area, rice-planting schedules, and tertiary irrigation system locations. These factors are crucial for verification and validation.

4.2. *Uncertainty of the study*

The use of machine learning may introduce biases and uncertainties in the evaluation results. Furthermore, in maximizing the potential of the GEE for parallel processing and analysis of geospatial data, the issue of data quality is a critical factor for robust monitoring and evaluation procedures. Common factors that affect data quality include irregular instrument visits, spatial scaling issues and cloud contamination (Weiss et al., 2020). Therefore, verification and validation of machine learning output with ground data are up most important. Besides, due to the limitation of global RS-ET datasets availability, this study only utilized three datasets. A reliance of RS-ET in this preliminary study is on MODIS-ET, which is known to provide global cumulative 8-day ET data at 0.5 km resolution. According to Sriwongsitanon et al. (2020), MODIS-ET would offer a promising application in the fields of hydrology, agronomy, and irrigation, especially in humid tropical climates. The selection of this dataset in this study, compared to TerraClimate-ET and FLDAS-ET, is assured that RS-ET can be collected at finer scale which is presented by the irrigation block level. The obtained values are also consistent with the existing literature, considering how difficult to measure actual ET in the field, especially to cover large-scale area. In addition, this dataset (MOD16A2GF) is not available in near real-time as

Table 5
The statistical distribution of crop water productivity (CWP) according to irrigation systems and scheduling phases.

	CWP of main season 2019 (kg m^{-3})						CWP of main season 2020 (kg m^{-3})					
	Phase 1		Phase 2		Phase 3		Phase 1		Phase 2		Phase 3	
	NTIS	TIS	NTIS	TIS	NTIS	TIS	NTIS	TIS	NTIS	TIS	NTIS	TIS
Maximum	1.38	1.22	1.28	1.24	1.37	1.22	1.41	1.28	1.45	1.33	1.39	1.38
Minimum	1.03	1.07	1.02	1.04	0.97	1.02	1.11	1.12	1.21	1.17	1.15	1.25
Median	1.13	1.11	1.20	1.07	1.18	1.15	1.24	1.26	1.26	1.24	1.24	1.32
	CWP of off-season 2019 (kg m^{-3})						CWP of off-season 2020 (kg m^{-3})					
	Phase 1		Phase 2		Phase 3		Phase 1		Phase 2		Phase 3	
	NTIS	TIS	NTIS	TIS	NTIS	TIS	NTIS	TIS	NTIS	TIS	NTIS	TIS
Maximum	1.25	1.17	1.25	1.22	1.44	1.21	1.13	1.11	1.35	1.23	1.31	1.21
Minimum	1.02	1.08	1.08	1.06	1.07	1.10	0.94	0.90	1.12	0.98	1.00	1.11
Median	1.13	1.15	1.13	1.12	1.21	1.15	1.07	0.99	1.18	1.15	1.15	1.21

Abbreviations: NTIS: non-tertiary irrigation system; TIS: tertiary irrigation system

the gap-filling process is required (Running et al., 2021). Properly processed cloud-free satellite imagery must be considered and a thorough investigation of the adequacy of the data is warranted. To generate the higher quality MOD16 ET, each contaminated pixel must be processed using the logic embedded in the MOD16 algorithm, and the final datasets are not available until the end of the year, with detailed explanations available in their latest user guide.

4.3. Future works

The outcomes of this study will guide future assessments of tertiary irrigation systems using processed remote sensing data. As higher resolution RS-ET datasets become available in GEE, the JavaScript code developed in this study will serve as a reference, simplifying the evaluation of tertiary irrigation system, thus, promoting sustainable monitoring.

Combining satellite sources with different revisit times and integrating data from various sensors ensures more frequent and reliable monitoring. Water withdrawal by farmers significantly impacts water allocation, affecting rice crop growth and providing valuable insights into water resource management (Baharudin and Arshad, 2015; Zhang et al., 2022). More frequent evaluations than monthly are recommended to effectively capture local management practices utilizing tertiary irrigation system for water withdrawal. While water withdrawal can be measured quantitively at intake level, the effectiveness of remote sensing data from Synthetic Aperture Radar (SAR) in monitoring water management practices has been demonstrated in several studies when in-situ data unavailable (El Hajj et al., 2022; Shorachi et al., 2022; Veloso et al., 2017). Spatial-temporal information from SAR data provides a valuable perspective in evaluating tertiary irrigation systems, such as assessing field plots' adherence to rice-planting schedules (Zahir et al., 2024). However, the use of SAR for tertiary irrigation system evaluation at regional scales remained underexplored. The freely available, high resolution (10 m for spatial, 12 days for temporal) Sentinel-1 SAR data in the GEE, offers a comprehensive understanding of the performance and water productivity of the irrigation system.

5. Conclusions

The results of our approach provided sufficient information on effectiveness of tertiary irrigation system from a regional perspective. Considering the difficulties of regular evaluation through a resource-intensive water balance approach in large scale area, the tertiary irrigation system blocks were evaluated using spatially collected RS-ET and downscaled yields from higher level statistics through NDVI. Based on the current water management strategies for the entire target period, the tertiary irrigation system in phase 1 shows remarkable performance in water distribution during the irrigation period. According to the equity indicator (threshold <10 %), the tertiary irrigation system has an excellent performance (2–8 %) in the off-season. However, throughout the target period, the equity phase 1 is between 3–10 %, followed by phase 2 (2–11 %) and phase 3 (2–13 %). For the adequacy indicator, the performance of tertiary irrigation system was relatively moderate throughout target period (threshold is >0.75), with phase 1 performing better (median: 0.67, maximum: 0.82), followed by phase 2 (median: 0.64, maximum: 0.80) and phase 3 (median: 0.60, maximum: 0.64). The water productivity indicator shows consistently good performance for the tertiary irrigation system in phase 1 and phase 3, while phase 2 fluctuates each season. Regular evaluations are recommended to monitor the performance of the tertiary irrigation system. The approach ensured that the process of regular monitoring and evaluation of the tertiary irrigation system was streamlined within a large-scale irrigation scheme and served as a key informant for authorities and farmers to efficiently plan corrective actions such as improving agricultural practices and water management strategies.

CRediT authorship contribution statement

Aliya Mhd Zahir: Writing – original draft, Visualization, Software, Methodology, Formal analysis, Data curation, Conceptualization, Investigation. **Hiroaki Somura:** Writing – review & editing, Validation, Supervision, Project administration, Methodology, Funding acquisition, Conceptualization, Resources, Investigation. **Toshitsugu Moroizumi:** Writing – review & editing, Supervision.

Declaration of Competing Interest

The authors declare that they have no known competing financial interests or personal relationships that could have appeared to influence the work reported in this paper.

Acknowledgements

This study was conducted under "Agriculture Study Network Program" supporting by Japan International Cooperation Agency (JICA) as a part of doctorate studies. The authors give credit to "NASA's Land Processes Distributed Active Archive Center (LP DAAC)" for dataset. The authors gratefully acknowledge the Muda Agricultural and Development Authority (MADA) and for providing information and support related to this study.

Data Availability

Data will be made available on request.

References

Abatzoglou, J.T., Dobrowski, S.Z., Parks, S.A., Hegewisch, K.C., 2018. TerraClimate, a high-resolution global dataset of monthly climate and climatic water balance from 1958–2015. Sci. Data 5, 170191. https://doi.org/10.1038/sdata.2017.191.

Ahmad, M.D., Turral, H., Nazeer, A., 2009. Diagnosing irrigation performance and water productivity through satellite remote sensing and secondary data in a large irrigation system of Pakistan. Agric. Water Manag. 96, 551–564. https://doi.org/10.1016/j.agwat.2008.09.017.

Akhtar, F., Awan, U., Tischbein, B., Liaqat, U., 2018. Assessment of irrigation performance in large river basins under data scarce environment—A Case of Kabul River Basin, Afghanistan. Remote Sens 10, 972. https://doi.org/10.3390/rs10060972.

Alberto, Ma.C.R., Wassmann, R., Hirano, T., Miyata, A., Hatano, R., Kumar, A., Padre, A., Amante, M., 2011. Comparisons of energy balance and evapotranspiration between flooded and aerobic rice fields in the Philippines. Agric. Water Manag. 98, 1417–1430. https://doi.org/10.1016/j.agwat.2011.04.011.

Baharudin, S.A., Arshad, F.M., 2015. Water management in the paddy area in MADA. Econ. Techn. Manag. Review 10, 21–29.

Basheer, S., Wang, X., Farooque, A.A., Nawaz, R.A., Liu, K., Adekanmbi, T., Liu, S., 2022. Comparison of land use land cover classifiers using different satellite imagery and machine learning techniques. Remote Sens 14, 4978. https://doi.org/10.3390/rs14194978.

Bastiaanssen, W.G.M., Bos, M.G., 1999. Irrigation performance indicators based on remotely sensed data: A review of literature. Irrig. Drain. Syst. 13, 291–311. https://doi.org/10.1023/A:1006355315251.

Bastiaanssen, W.G.M., Van Der Wal, T., Visser, T.N.M., 1996. Diagnosis of regional evaporation by remote sensing to support irrigation performance assessment. Irrig. Drain. Syst. 10, 1–23. https://doi.org/10.1007/BF01102762.

Blatchford, M.L., Mannaerts, C.M., Zeng, Y., Nouri, H., Karimi, P., 2019. Status of accuracy in remotely sensed and in-situ agricultural water productivity estimates: A review. Remote Sens. Environ. 234, 111413. https://doi.org/10.1016/j.rse.2019.111413.

Bos, M.G., Burton, M.A., Molden, D.J., 2005. Irrigation and Drainage Performance Assessment: Practical Guidelines. CABI Publishing, Wallingford, UK.

Bos, M.G., Murray-Rust, D.H., Merrey, D.J., Johnson, H.G., Snellen, W.B., 1994. Methodologies for assessing performance of irrigation and drainage management. Irrig. Drain. Syst. 7, 231–261. https://doi.org/10.1007/BF00881553.

Cabangon, R.J., Tuong, T.P., Abdullah, N.B., 2002. Comparing water input and water productivity of transplanted and direct-seeded rice production systems. Agric. Water Manag. 57, 11–31. https://doi.org/10.1016/S0378-3774(02)00048-3.

Cai, X.L., Sharma, B.R., 2010. Integrating remote sensing, census and weather data for an assessment of rice yield, water consumption and water productivity in the Indo-Gangetic river basin. Agric. Water Manag. 97, 309–316. https://doi.org/10.1016/j.agwat.2009.09.021.

Calera, A., Campos, I., Osann, A., D'Urso, G., Menenti, M., 2017. Remote sensing for crop water management: from ET modelling to services for the end users. Sensors 17, 1–25. https://doi.org/10.3390/s17051104.

Chen, N., Yu, L., Zhang, X., Shen, Y., Zeng, L., Hu, Q., Niyogi, D., 2020. Mapping paddy rice fields by combining multi-temporal vegetation index and synthetic aperture radar remote sensing data using Google Earth Engine machine learning platform. Remote Sens 12, 2992. https://doi.org/10.3390/rs12182992.

Conrad, C., Usman, M., Morper-Busch, L., Schönbrodt-Stitt, S., 2020. Remote sensing-based assessments of land use, soil and vegetation status, crop production and water use in irrigation systems of the Aral Sea Basin. A review. Water Secur 11, 100078. https://doi.org/10.1016/j.wasec.2020.100078.

Deines, J.M., Kendall, A.D., Crowley, M.A., Rapp, J., Cardille, J.A., Hyndman, D.W., 2019. Mapping three decades of annual irrigation across the US High Plains Aquifer using Landsat and Google Earth Engine. Remote Sens. Environ. 233, 111400. https://doi.org/10.1016/j.rse.2019.111400.

Deines, J.M., Kendall, A.D., Hyndman, D.W., 2017. Annual irrigation dynamics in the U. S. northern high plains derived from landsat satellite data. Geophys. Res. Lett. 44, 9350–9360. https://doi.org/10.1002/2017GL074071.

El Hajj, M.M., Almashharawi, S.K., Johansen, K., Elfarkh, J., McCabe, M.F., 2022. Exploring the use of synthetic aperture radar data for irrigation management in super high-density olive orchards. Int. J. Appl. Earth Obs. Geoinf. 112. https://doi.org/10.1016/j.jag.2022.102878.

Elnashar, A., Wang, L., Wu, B., Zhu, W., Zeng, H., 2021. Synthesis of global actual evapotranspiration from 1982 to 2019. Earth Syst. Sci. Data 13, 447–480. https://doi.org/10.5194/essd-13-447-2021.

Elshaikh, A.E., Jiao, X., Yang, S. hong, 2018. Performance evaluation of irrigation projects: theories, methods, and techniques. Agric. Water Manag. 203, 87–96. https://doi.org/10.1016/j.agwat.2018.02.034.

Fatchurrachman, Rudiyanto, Soh, N.C., Shah, R.M., Giap, S.G.E., Setiawan, B.I., Minasny, B., 2022. High-resolution mapping of paddy rice extent and growth stages across Peninsular Malaysia using a fusion of Sentinel-1 and 2 time series data in Google Earth Engine. Remote Sens 14, 1875. https://doi.org/10.3390/rs14081875.

Feizizadeh, B., Omarzadeh, D., Kazemi Garajeh, M., Lakes, T., Blaschke, T., 2023. Machine learning data-driven approaches for land use/cover mapping and trend analysis using Google Earth Engine. J. Environ. Plan. Manag. 66, 665–697. https://doi.org/10.1080/09640568.2021.2001317.

Franklin, J., 1995. Predictive vegetation mapping: Geographic modelling of biospatial patterns in relation to environmental gradients. Prog. Phys. Geog. Earth Environ. 19, 474–499. https://doi.org/10.1177/030913339501900403.

Fujii, H., Cho, M.C., Kitamura, Y., 1993. Differences in presaturation progress and water requirements between areas with and without tertiary canals - case study in the Muda Irrigation Project area, Malaysia, 1993 J. Irrig. Eng. Rural Plan 16–30. https://doi.org/10.11408/jierp1982.1993.25_16.

GEE, 2022. Morphological Operations from Google Earth Engine Guides. ⟨https://developers.google.com/earth-engine/guides/image_morph⟩ (accessed 17 August.22).

Gorelick, N., Hancher, M., Dixon, M., Ilyushchenko, S., Thau, D., Moore, R., 2017. Google Earth Engine: Planetary-scale geospatial analysis for everyone. Remote Sens. Environ. 202, 18–27. https://doi.org/10.1016/j.rse.2017.06.031.

Hanafiah, M.M., Ghazali, N.F., Harun, S.N., Abdulaali, H.S., Abdul Hasan, M.J., Amri Kamarudin, M.K., 2019. Assessing water scarcity in Malaysia: A case study of rice production. Desalin. Water Treat. 149, 274–287. https://doi.org/10.5004/dwt.2019.23841.

Jensen, M.E., Burman, R.D., Allen, R.G., 1990. Evapotranspiration and irrigation water requirements. ASCE.

Jindo, K., Kozan, O., Iseki, K., Maestrini, B., van Evert, F.K., Wubengeda, Y., Arai, E., Shimabukuro, Y.E., Sawada, Y., Kempenaar, C., 2021. Potential utilization of satellite remote sensing for field-based agricultural studies. Chem. Biol. Technol. Agric. 8, 58. https://doi.org/10.1186/s40538-021-00253-4.

Karimi, P., Bongani, B., Blatchford, M., de Fraiture, C., 2019. Global satellite-based ET products for the local level irrigation management: an application of irrigation performance assessment in the sugarbelt of Swaziland. Remote Sens 11, 705. https://doi.org/10.3390/rs11060705.

Kharrou, M.H., Le Page, M., Chehbouni, A., Simonneaux, V., Er-Raki, S., Jarlan, L., Ouzine, L., Khabba, S., Chehbouni, G., 2013. Assessment of equity and adequacy of water delivery in irrigation systems using remote sensing-based indicators in semi-arid region, Morocco. Water Resour. Manag. 27, 4697–4714. https://doi.org/10.1007/s11269-013-0438-5.

Kharrou, M.H., Simonneaux, V., Er-raki, S., Page, M., Le, Khabba, S., Chehbouni, A., 2021. Assessing irrigation water use with remote sensing-based soil water balance at an irrigation scheme level in a semi-arid region of morocco. Remote Sens 13, 1–22. https://doi.org/10.3390/rs13061133.

Kitamura, Y., 1988. Water balance in a tertiary development area with low and flat paddy land - case study in Muda Irrigation Project area, Malaysia. Irrig. Eng. Rural Plan. https://doi.org/10.11408/jierp1982.1988.18.

Kitamura, Y., 1990. Management of irrigation systems for rice double cropping culture in the tropical monsoon area (No. No. 27). Tropical Agricultural Research Center, Ibaraki, Japan.

Laipelt, L., Henrique Bloedow Kayser, R., Santos Fleischmann, A., Ruhoff, A., Bastiaanssen, W., Erickson, T.A., Melton, F., 2021. Long-term monitoring of evapotranspiration using the SEBAL algorithm and Google Earth Engine cloud computing. ISPRS J. Photogramm. Remote Sens. 178, 81–96. https://doi.org/10.1016/j.isprsjprs.2021.05.018.

MADA, 2023. Pengenalan Pertubuhan Peladang Kawasan (PPK). ⟨https://www.mada.gov.my/?q=4501⟩ (accessed 29 September.2023).

Malaymail, 2020. Kedah paddy farmers hit hard by hot weather. ⟨https://www.malaymail.com/news/malaysia/2020/01/13/kedah-paddy-farmers-hit-hard-by-hot-weather/1827612⟩ (accessed 25 October.2022).

McFeeters, S.K., 1996. The use of the Normalized Difference Water Index (NDWI) in the delineation of open water features. Int. J. Remote Sens. 17, 1425–1432. https://doi.org/10.1080/01431169608948714.

McNally, A., Arsenault, K., Kumar, S., Shukla, S., Peterson, P., Wang, S., Funk, C., Peters-Lidard, C.D., Verdin, J.P., 2017. A land data assimilation system for sub-Saharan Africa food and water security applications. Sci. Data 4, 170012. https://doi.org/10.1038/sdata.2017.12.

Mohammadi, A., Parvaresh Rizi, A., Abbasi, N., 2019. Field measurement and analysis of water losses at the main and tertiary levels of irrigation canals: Varamin Irrigation Scheme, Iran. Glob. Ecol. Conserv. 18. https://doi.org/10.1016/J.GECCO.2019.E00646.

Mohsen Aly, A., Kitamura, Y., Shimizu, K., 2013. Assessment of irrigation practices at the tertiary canal level in an improved system—a case study of Wasat area, the Nile Delta. Paddy Water Environ. 11, 445–454. https://doi.org/10.1007/s10333-012-0335-1.

Mu, Q., Heinsch, F.A., Zhao, M., Running, S.W., 2007. Development of a global evapotranspiration algorithm based on MODIS and global meteorology data. Remote Sens. Environ. 111, 519–536. https://doi.org/10.1016/j.rse.2007.04.015.

Mu, Q., Zhao, M., Running, S.W., 2011. Improvements to a MODIS global terrestrial evapotranspiration algorithm. Remote Sens. Environ. 115, 1781–1800. https://doi.org/10.1016/j.rse.2011.02.019.

Nazuri, N.S., Man, N., 2016. Acceptance and practices on new paddy seed variety among farmers in MADA granary area. Acad. J. Inter. Stud. https://doi.org/10.5901/ajis.2016.v5n2p105.

Poudel, U., Stephen, H., Ahmad, S., 2021. Evaluating irrigation performance and water productivity using EEFlux ET and NDVI. Sustainability 13, 7967. https://doi.org/10.3390/su13147967.

Ragab, M.F.S., Shimizu, K., Abou El Hassan, W.H., Nakumura, K., Watanabe, T., 2019. Investigation of irrigation performance at the tertiary canal level in the Nile Delta of Egypt. Paddy Water Environ. 17, 69–74. https://doi.org/10.1007/s10333-019-00698-2.

Rodriguez-Galiano, V.F., Ghimire, B., Rogan, J., Chica-Olmo, M., Rigol-Sanchez, J.P., 2012. An assessment of the effectiveness of a random forest classifier for land-cover classification. ISPRS J. Photogramm. Remote Sens. 67, 93–104. https://doi.org/10.1016/j.isprsjprs.2011.11.002.

Roerink, G.J., Bastiaanssen, W.G.M., Chambouleyron, J., Menenti, M., 1997. Relating crop water consumption to irrigation water supply by remote sensing, 11 Water Resour. Manag. 11 (6), 445–465. https://doi.org/10.1023/A:1007982411718.

Rowshon, M.K., Mojid, M.A., Amin, M.S.M., Azwan, M., Yazid, A.M., 2014. Improving Irrigation Water Delivery Performance of a Large-Scale Rice Irrigation Scheme. J. Irrig. Drain. Eng. 140, 04014027. https://doi.org/10.1061/(ASCE)IR.1943-4774.0000747.

Rudiyanto, Minasny, B., Shah, R.M., Soh, N.C., Arif, C., Setiawan, B.I., 2019. Automated near-real-time mapping and monitoring of rice extent, cropping patterns, and growth stages in Southeast Asia using Sentinel-1 time series on a Google Earth Engine platform. Remote Sens 11, 1–27. https://doi.org/10.3390/rs11141666.

Running, S.W., Mu, Q., Zhao, M., Moreno, A., 2021. MODIS Global Terrestrial Evapotranspiration (ET) Product (MOD16A2/A3 and Year-end Gap-filled MOD16A2GF/A3GF) NASA Earth Observing System MODIS Land Algorithm (For Collection 6.1).

Rusli, N.M., Zainon Noor, Z., Mat Taib, S., Salehan, N., Sabli, M., 2022. Water footprint of rice production in Malaysia: A review of evapotranspiration and factors of climate change for rice and food security in Malaysia. Malays. J. Fund. Appl. Sci. 18, 497–510. https://doi.org/10.11113/mjfas.v18n4.2601.

Sawadogo, A., Kouadio, L., Traoré, F., Zwart, S.J., Hessels, T., Gündoğdu, K.S., 2020. Spatiotemporal assessment of irrigation performance of the Kou Valley Irrigation Scheme in Burkina Faso using satellite remote sensing-derived indicators. ISPRS Int. J. Geoinf. 9, 484. https://doi.org/10.3390/ijgi9080484.

Seiro, I., Satoshi, O., Kazunari, T., 2016. Impacts of tertiary canal irrigation: impact evaluation of an infrastructure project. Institute of Developing Economies. Jpn. Extern. Trade Organ. (JETRO). https://doi.org/10.20561/00037585.

Sekaran, R., 2020. Kedah starts cloud seeding operations. ⟨https://www.thestar.com.my/news/nation/2020/01/20/kedah-starts-cloud-seeding-operations⟩ (accessed 25 October.2022).

Shaharum, N.S.N., Shafri, H.Z.M., Ghani, W.A.W.A.K., Samsatli, S., Al-Habshi, M.M.A., Yusuf, B., 2020. Oil palm mapping over Peninsular Malaysia using Google Earth Engine and machine learning algorithms. Remote Sens. Appl. 17, 100287. https://doi.org/10.1016/j.rsase.2020.100287.

Shetty, S., Gupta, P.K., Belgiu, M., Srivastav, S.K., 2021. Assessing the effect of training sampling design on the performance of machine learning classifiers for land cover mapping using multi-temporal remote sensing data and Google Earth Engine. Remote Sens 13, 1433. https://doi.org/10.3390/rs13081433.

Shirsath, P.B., Sehgal, V.K., Aggarwal, P.K., 2020. Downscaling regional crop yields to local scale using remote sensing. Agriculture 10, 58. https://doi.org/10.3390/agriculture10030058.

Shorachi, M., Kumar, V., Steele-Dunne, S.C., 2022. Sentinel-1 SAR Backscatter Response to Agricultural Drought in The Netherlands. Remote Sens 14. https://doi.org/10.3390/rs14102435.

Sriwongsitanon, N., Suwawong, T., Thianpopirug, S., Williams, J., Jia, L., Bastiaanssen, W., 2020. Validation of seven global remotely sensed ET products across Thailand using water balance measurements and land use classifications. J. Hydrol. Reg. Stud. 30, 100709. https://doi.org/10.1016/j.ejrh.2020.100709.

Syed, N.S.B., Shuqi, Z., Babar, M.M., Soothar, R.K., 2021. Analysis of Conveyance Losses from Tertiary Irrigation Network. Civ. Eng. J. 7, 1731–1740. https://doi.org/10.28991/cej-2021-03091756.

Thakur, A.K., Mandal, K.G., Mohanty, R.K., Ambast, S.K., 2018. Rice root growth, photosynthesis, yield and water productivity improvements through modifying cultivation practices and water management. Agric. Water Manag. 206, 67–77. https://doi.org/10.1016/j.agwat.2018.04.027.

Tukimat, N.N.A., Harun, S., Shahid, S., 2012. Comparison of different methods in estimating potential evapotranspiration at Muda Irrigation Scheme of Malaysia. J. Agr. Rural Dev. Trop. Subtrop 113, 77–85.

Tukimat, N.N.A., Harun, S., Shahid, S., 2017. Modeling Irrigation Water Demand in a Tropical Paddy Cultivated Area in the Context of Climate Change. J Water Resour. Plan. Manag. 143, 05017003. https://doi.org/10.1061/(ASCE)WR.1943-5452.0000753.

Usman, M., Liedl, R., Shahid, M.A., 2014. Managing irrigation water by yield and water productivity assessment of a rice-wheat system using remote sensing. J. Irrig. Drain. Eng. 140, 04014022. https://doi.org/10.1061/(ASCE)IR.1943-4774.0000732.

Vandersypen, K., Bengaly, K., Keita, A.C.T., Sidibe, S., Raes, D., Jamin, J.Y., 2006. Irrigation performance at tertiary level in the rice schemes of the Office du Niger (Mali): adequate water delivery through over-supply. Agric. Water Manag. 83, 144–152. https://doi.org/10.1016/j.agwat.2005.11.003.

Veloso, A., Mermoz, S., Bouvet, A., Le Toan, T., Planells, M., Dejoux, J.F., Ceschia, E., 2017. Understanding the temporal behavior of crops using Sentinel-1 and Sentinel-2-like data for agricultural applications. Remote Sens. Environ. 199, 415–426. https://doi.org/10.1016/j.rse.2017.07.015.

Weiss, M., Jacob, F., Duveiller, G., 2020. Remote sensing for agricultural applications: a meta-review. Remote Sens. Environ. 236, 111402. https://doi.org/10.1016/j.rse.2019.111402.

Xie, Y., Lark, T.J., Brown, J.F., Gibbs, H.K., 2019. Mapping irrigated cropland extent across the conterminous United States at 30m resolution using a semi-automatic training approach on Google Earth Engine. ISPRS J. Photogramm. Remote Sens. 155, 136–149. https://doi.org/10.1016/j.isprsjprs.2019.07.005.

Xu, H., 2006. Modification of normalised difference water index (NDWI) to enhance open water features in remotely sensed imagery. Int. J. Remote Sens. 27, 3025–3033. https://doi.org/10.1080/01431160600589179.

Yashima, S., 1982. Water balance in low and flat paddy land: A case study in the Muda Irrigation Project area, Malaysia. JARQ (Japan).

Yashima, S., 1987. Water balance for rice double cropping in the Muda area, Malaysia. Tropical agriculture research series 20, 130–138.

Zahir, A.M., Somura, H., Moroizumi, T., 2024. Efficient agricultural monitoring: a methodology for assessing individual farmer adherence to rice-planting schedule for tertiary irrigation system under the Muda Irrigation Scheme using Earth observation datasets. Hydrol. Res. Lett. 18, 14–21. https://doi.org/10.3178/hrl.18.14.

Zha, Y., Gao, J., Ni, S., 2003. Use of normalized difference built-up index in automatically mapping urban areas from TM imagery. Int. J. Remote Sens. 24, 583–594. https://doi.org/10.1080/01431160304987.

Zhang, L., Zheng, D., Zhang, K., Chen, H., Ge, Y., Li, X., 2022. Divergent trends in irrigation-water withdrawal and consumption over mainland China. Environ. Res. Lett. 17, 094001. https://doi.org/10.1088/1748-9326/ac8606.

Zhang, Y., Kong, D., Gan, R., Chiew, F.H.S., McVicar, T.R., Zhang, Q., Yang, Y., 2019. Coupled estimation of 500m and 8-day resolution global evapotranspiration and gross primary production in 2002–2017. Remote Sens. Environ. 222, 165–182. https://doi.org/10.1016/j.rse.2018.12.031.

Zhao, H., Yang, C., Guo, W., Zhang, L., Zhang, D., 2020. Automatic estimation of crop disease severity levels based on vegetation index normalization. Remote Sens 12, 1930. https://doi.org/10.3390/rs12121930.

Zheng, H., Cheng, T., Yao, X., Deng, X., Tian, Y., Cao, W., Zhu, Y., 2016. Detection of rice phenology through time series analysis of ground-based spectral index data. Field Crops Res 198, 131–139. https://doi.org/10.1016/j.fcr.2016.08.027.

Zurqani, H.A., Allen, J.S., Post, C.J., Pellett, C.A., Walker, T.C., 2021. Mapping and quantifying agricultural irrigation in heterogeneous landscapes using Google Earth Engine. Remote Sens. Appl. 23, 100590. https://doi.org/10.1016/j.rsase.2021.100590.

Zwart, S.J., Bastiaanssen, W.G.M., 2004. Review of measured crop water productivity values for irrigated wheat, rice, cotton and maize. Agric. Water Manag. 69, 115–133. https://doi.org/10.1016/j.agwat.2004.04.007.

Zwart, S.J., Bastiaanssen, W.G.M., 2007. SEBAL for detecting spatial variation of water productivity and scope for improvement in eight irrigated wheat systems. Agric. Water Manag. 89, 287–296. https://doi.org/10.1016/j.agwat.2007.02.002.

Zwart, S.J., Leclert, L.M.C., 2010. A remote sensing-based irrigation performance assessment: a case study of the Office du Niger in Mali. Irrig. Sci. 28, 371–385. https://doi.org/10.1007/s00271-009-0199-3.